Quench Prediction for NI REBCO Pancake Coils Using LSTM

Yusuke Nakai and So Noguchi

***Abstract*—In this paper, we propose a neural network-based quench prediction method. High-temperature superconductors (HTS) has a slower propagation velocity in the local normal-zone than low-temperature superconductors (LTS), and the hotspots are more likely to occur. The cases of coil burnout due to this have been reported, and such quenches are difficult to detect. Several methods have been proposed to detect and protect against quenches, but the coil temperature is already rising when a quench is detected. This means that coil operation must be stopped before the actual quench signal by predicting the occurrence of a quench. In this study, we show the results of quench prediction for unknown data by training data obtained from numerical simulations using a neural network called LSTM.**

***Index Terms*—REBCO pancake coils, quench prediction, neural network, LSTM.**

I. INTRODUCTION

REBCO (rare-earth barium copper oxide), a 2nd-generation high-temperature superconductor, has excellent high-current characteristics, and it is expected to be applied to magnets for generation of high magnetic fields [1]-[3]. When a local normal transition occurs in a REBCO coil, the REBCO coil may burn out due to a thermal runaway. The local normal zone of a REBCO tape propagates much slower than that of low-temperature superconductors [4]. It is, therefore, difficult to detect such local normal-zone propagation in a REBCO tape. Consequently, the normal zone rapidly widens due to high joule heat. Some methods to detect a local normal state transition or a quench have been proposed; e.g., targeting voltage, acoustic, and heat generated in normal-state-transitioned/quenched coils [5]-[7].

The no-insulation (NI) winding technique [8] has been proposed to improve the thermal stability of REBCO pancake coils. As a monumental work, the world record 45.5 T DC field was achieved by the NI winding technique applying to an insert REBCO magnet [9]. After 45.5 T generation, the insert REBCO magnet has quenched, but not burned out. Meanwhile, the toroidal field test magnet of the plasma science and fusion center, MIT was burned out during its quench test [10]. It is occasionally unsuccessful to detect a local normal state transition or a quench immediately after its occurrence, or a normal-state-transitioned/quenched coil cannot be prevented from burning-out. Toward practical applications of high magnetic field REBCO magnets, an effective quench detection technique must be developed.

As one quench detection method, it is, therefore, desired to predict a local normal state transition in advance, and the operating current would be able to shut down safely before a quench occurs. In this study, we utilize a LSTM (long short-term memory) for quench prediction. The LSTM is a kind of neural network, and it is used for forecasting time-series data [11]-[13]. The input to the LSTM is a set of continuous time-series data, and the output is the predicted values at the following time. In the proposed system, the coil voltages obtained from numerical simulations are inputted as training data. From the data, the LSTM learns whether the coil voltage rises rapidly or does not, and voltages are predicted in the following time values. When a quench is successfully predicted in this way, the REBCO coil can be protected safely from performance deterioration or coil burn-out.

II. NUMERICAL SIMULATION

A. Simulation Model

The coil voltage data used in the training are obtained through numerical simulations in this first trial. A no-insulation (NI) REBCO pancake coil is represented by an equivalent circuit as shown in Fig. 1. Since many cases should be simulated to make the coil voltage data, a simple numerical simulation model [14] is employed. The single pancake coil is divided in the radial direction, and each element is represented as an equivalent circuit connecting in series each other. Fig. 1 shows radially divided coil (upper) and the circumferential

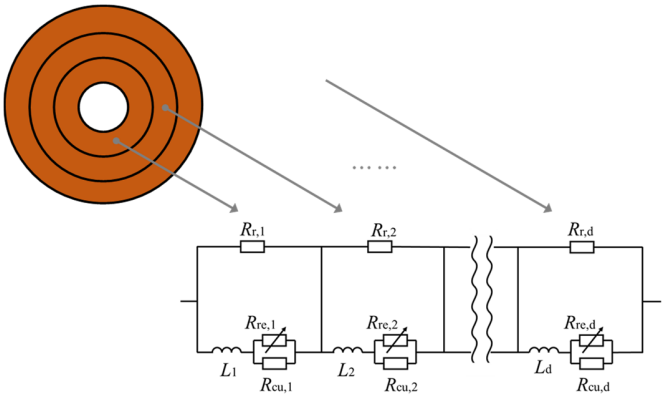

Fig. 1. Equivalent circuit.

Manuscript received. This work was supported by the JSPS KAKENHI under Grant No. 20H02125. (*Corresponding author: So Noguchi.*)

Y. Nakai and S. Noguchi were with Graduate School of Information Science and Technology, Hokkaido University, Sapporo, 060-0814 Japan (e-mail: y_nakai@em.ist.hokudai.ac.jp, noguchi@ssi.ist.hokudai.ac.jp).

Color versions of one or more of the figures in this article are available online at http://ieeexplore.ieee.org

Digital Object Identifier will be inserted here upon acceptance.

equivalent circuit elements (lower). In this way, the NI REBCO coil is expressed in low dimensions to shorten the computation time. The current behaviors are obtained solving (1)-(3), and the coil voltages are computed from these results.

$$R_{\mathrm{cu},i}I_{\mathrm{cu},i} - R_{\mathrm{re},i}I_{\mathrm{re},i} = 0 \quad (1)$$

$$R_{\mathrm{cu},i}I_{\mathrm{cu},i} - R_{\mathrm{r},i}I_{\mathrm{r},i} + \sum_{j=1}^{d} L_{i,j}\frac{d\left(I_{\mathrm{re},j} + I_{\mathrm{cu},j}\right)}{dt} = 0 \quad (2)$$

$$I_{\mathrm{r},i} + I_{\mathrm{re},i} + I_{\mathrm{cu},i} - I_{\mathrm{op}} = 0 \quad (3)$$

where i, d, and t are the element number, the number of radial divisions, and the time, respectively. I_{re}, I_{cu}, I_r, and I_{op} are the REBCO layer current, the copper layer current, the radial current, and the operating current, respectively. R_{re}, R_{cu}, R_r, and L are the REBCO layer resistance, the copper layer resistance, the radial contact resistance, and the inductance. Here, the REBCO layer resistance R_{re} is computed from the n-power index model depending on the temperature, the field intensity and angle [15].

Together with the circuit simulation, the thermal finite element analysis (FEA) is coupled. Here, for simplicity, the adiabatic condition is applied. The coil temperature is reflected to the electric properties such as the resistivity. In this paper, the coil temperature is not used for the training of LTSM but will be used in the near future.

B. Simulation condition

With a constant current of 50 A flowing in an NI single pancake coil, a small external heat is continually applied to the mid-turns of the coil. As the external heat keeps adding from $t = 1$ s, a normal state transition occurs with the increase of the coil voltage and temperature. Fig. 2 shows the examples of voltage data used as training data. As the time passes, the heat spreads from the center elements to the inner/outer elements. Different voltage waveforms can be obtained changing the amount of the external heat.

Table I lists the specifications of the REBCO tape and coil on the numerical simulation. When the normal-state transition criterion is 10 μV/cm [16], the coil normal-state transition criterion is 0.05 V. Since the NI winding technique is applied for the test NI REBCO coil, it would not reach to quench even beyond the criterion voltage. As shown in Fig. 3, the coil

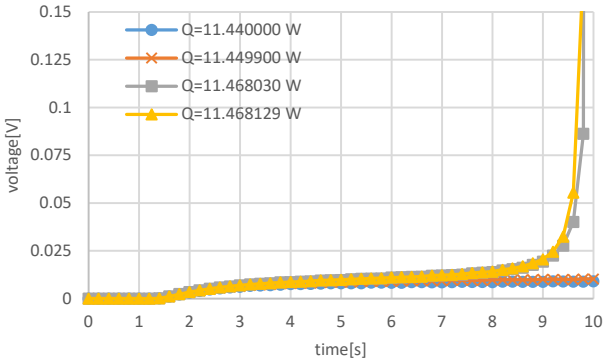

Fig. 2. Examples of the training data.

TABLE I
SPECIFICATIONS OF REBCO TAPE AND COIL

Parameters	Value
REBCO Tape	
Tape width [mm]	4.02
Tape thickness [mm]	0.1
REBCO layer thickness [mm]	1.0
Copper layer thickness [mm]	10.0
Critical temperature [K]	85
I_c @ 77K, self-field [A]	150.0
Coil	
Number of pancakes	1
Number of turns	200
I.D. / O.D. [mm]	60.0 / 100.0
Number of main coil divisions	10

TABLE II
SIMULATION CONDITIONS AND LEARNING CONDITIONS

Parameters	Value
Simulation Conditions	
Simulation time [s]	10
Time step [s]	0.01
Operating current [A]	50
Operating temperature [T]	77
Maximum heat transfer coefficient [W/(K·m^{-2})]	10000
External heat [W]	11.440000~11.449900, 11.468129~11.468030
Learning Conditions	
Number of data	200
training: Test	7: 3
Epochs	50
Batch size	100
Length of input data	10
Length of output data	100

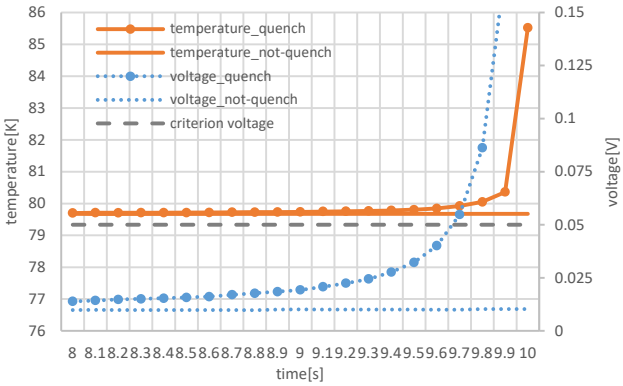

Fig. 3. Temperatures and voltages for quench and not-quench cases.

voltage may exceed the criterion voltage of 0.05 V before the temperature some element in the coil exceeds the critical temperature of 85 K. In this study, we have determined that a quench occurred when the critical temperature was exceeded.

Table II lists the numerical simulation conditions to generate the training data. Here, it is assumed that the test NI REBCO coil is cooled with the heat transfer coefficient of up to 10 KW·K^{-1}·m^{-2} [17].

III. LSTM

The LSTM (long short-term memory) [18] is a kind of neural network that can learn long-term dependencies. The

RNN (recurrent neural network), a similar type of neural network, passes information obtained once through data to subsequent ones with the next input; however, it has a problem of not being able to maintain the past information up to the present. The further apart the relevant information and the scene in which it is needed, the less the RNN is able to learn to associate the information. The LSTM improves on this problem. Figure 4 shows the structure of LSTM. The intermediate layer connecting the input and the output layers has a forget gate, an input gate, and an output gate. First, the forget gate computes the function f_t to determine which information is forgotten from cell state C_{t-1}.

$$f_t = \sigma\left(W_f \cdot [y_{t-1}, x_t] + b_f\right) \quad (4)$$

where W and b represent the weight and the bias in each gate, respectively. σ is a sigmoid function, using the new input x_t and the previous output y_{t-1}. '1' means keep the information completely, and '0' means discard the information in this sigmoid function. Next, the information is updated at the input gate. As before, x_t and y_{t-1} are used to compute i_t and the candidate value $\widetilde{C_t}$ to add to the cell state.

$$i_t = \sigma(W_i \cdot [y_{t-1}, x_t] + b_i) \quad (5)$$
$$\widetilde{C_t} = \tanh(W_c \cdot [y_{t-1}, x_t] + b_c) \quad (6)$$

The old cell state C_{t-1} is then multiplied by f_t to forget the information it does not need, and a new cell state C_t is generated by adding it multiplied by $\widetilde{C_t}$.

$$C_t = f_t * C_{t-1} + i_t * \widetilde{C_t} \quad (7)$$

Finally, the output gate calculates o_t and multiplies it by the processed cell state to determine what to output.

$$o_t = \sigma(W_0 \cdot [y_{t-1}, x_t] + b_0) \quad (8)$$
$$y_t = o_t * \tanh(C_t) \quad (9)$$

In (9), tanh is used to output only the portion determined by the sigmoid function. Following these steps, the LSTM updates its cell state and gradually changes its long-term memory while using the past output as the next input. Due to its excellent long-term memory characteristics, the LSTM has been applied to speech recognition and stock price prediction [19]-[20].

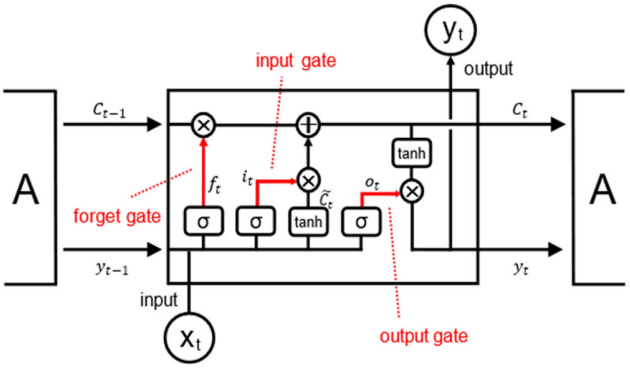

Fig. 4. The structure of LSTM.

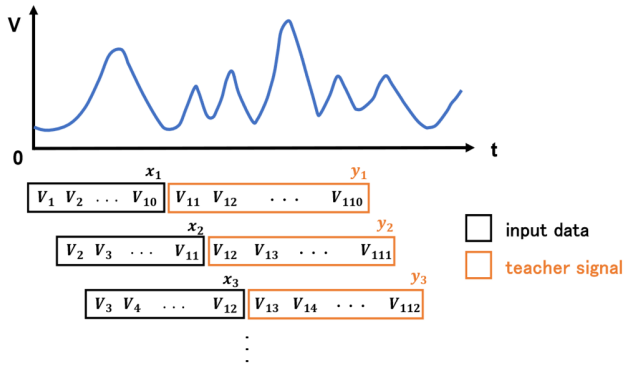

Fig. 5. How to create datasets.

IV. Prediction Results

When training, continuous time-series data with an arbitrary number of steps is used as input, and subsequent values are used as the teacher signal. With reference to these teacher signals, predictions are made for unknown inputs. In the present case, for each voltage waveform, the teacher signals are the 100 steps that follow when 10 steps of voltage are used as input. As shown in Fig. 5, many such data sets are generated by shifting the time. Table II shows the learning conditions. In Table II, "epoch" is the number of learning times and "batch size" is the size of one group when training data is divided into small group. During each learning session, instead of leaning all the data at once, the data is divided into small groups and learned in batch sizes. The performance improvement of the model is attributed to the optimization of these parameters, which are modified based on the loss function computed during training. In this study, MAE (Mean Absolute Error) is used as the loss function.

Figures 6 and 7 show the 1-second prediction results from t = 7 s, 8 s and 9 s for the voltage waveform, where the orange and blue broken curves show the 1-second predicted voltage and the voltage to be simulated. The blue broken curves with triangles are the input values used to predict each time. Here, the voltage to be predicted is not included in the training data. The input is the simulated voltage from 1 second before the start of each prediction. Figure 6 shows the voltage prediction results for a quench occurrence case; meanwhile, Fig. 7 shows the prediction results for a not-quench case. Although there are voltage noises, the voltage rises can be predicted well. In this study, we suppose that it is sufficient to know whether a quench occurs or not. However, the predicted values contain noise, and the values fluctuate. Increasing the prediction interval time reduces the noise but increases the possibility of false predictions. In this study, our priority is to avoid missing a quench detection.

V. Conclusion

We have studied a method for prediction of a quench event of REBCO coils using the LSTM. It is possible to predict the voltage rise that is a sign of quench before it would occur. We

can stop the coil operation in advance. However, it is still difficult to learn the voltage rise as a sign of quench because the voltage is small. In addition, 1 second is too short to take a quench protection, and the real voltage signal is noisy. We need to develop an AI quench prediction method much more.

As the next step, we will apply the develop method to a real NI REBCO pancake coil.

REFERENCES

[1] S. Yokoyama, *et al.*, "Research and development of the high stable magnet field ReBCO coil system fundamental technology for MRI," *IEEE Trans. Appl. Supercond.*, vol. 27, no. 4, Jun. 2017, Art. no. 4400604.
[2] K. Mizuno, *et al.*, "Experimental Production of a Real-Scale REBCO Magnet Aimed at Its Application to Maglev," *IEEE Trans. Appl. Supercond.*, vol. 27, no. 4, Jun. 2017, Art. no. 3600205.
[3] S. Takayama, *et al.*, "Development of an HTS Accelerator Magnet With REBCO Coils for Tests at HIMAC Beam Line," *IEEE Trans. Appl. Supercond.*, vol. 29, no. 5, Aug. 2019, Art. no. 4004205.
[4] Y. Yanagisawa, *et al.,* "The mechanism of thermal runaway due to continuous local disturbances in the YBCO-coated conductor coil winding," *Supercond. Sci. Technol.*, vol. 25, no.7, Jun. 2012, Art. no. 075014.
[5] J. M. Pfotenhauer, *et. al.*, "Voltage Detection and Magnet Protection," *IEEE Trans. Appl. Supercond.*, vol. 3, no. 1, Mar. 1993, pp. 273-276.
[6] H. Lee, *et al.*, "Detection of 'Hot Spots' in HTS Coils and Test Samples With Acoustic Emission Signals," *IEEE Trans. Appl. Supercond.*, vol. 14, no. 2, Jun. 2004, Art. no. 1298.
[7] F. Scurti, *et al.*, "Quench detection for high temperature superconductor magnets: a novel technique based on Rayleigh-backscattering interrogated optical fibers," *Supercond. Sci. Technol.*, vol. 29, no. 3, Jan. 2016, 03LT01.
[8] S. Hahn, D. K. Park, J. Bascuñán, and Y. Iwasa, "HTS Pancake Coils without Turn-to-Turn Insulation," *IEEE Trans. Appl. Supercond.*, vol. 21, no. 3, pp. 1592–1595, 2011.
[9] S. Hahn et al., "45.5-Tesla Direct-Current Magnetic Field Generated with a High-Temperature Superconducting Magnet," *Nature*, vol. 570, no.

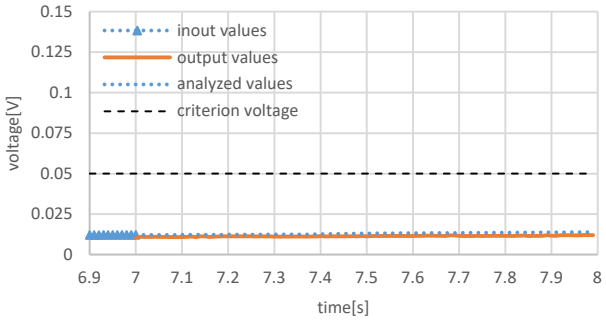

(a)

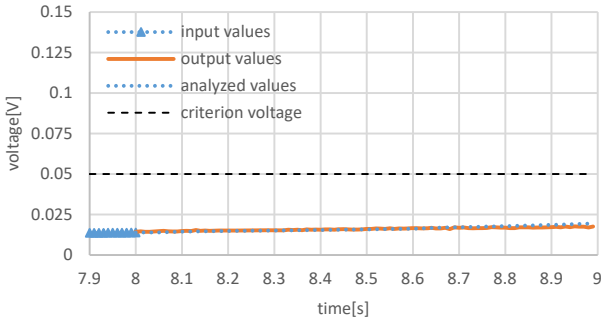

(b)

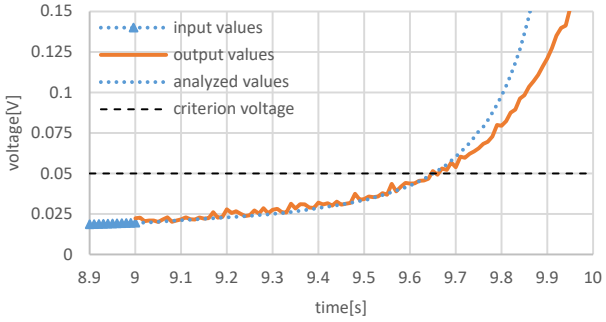

(c)

Fig. 6. Prediction for a quench case.

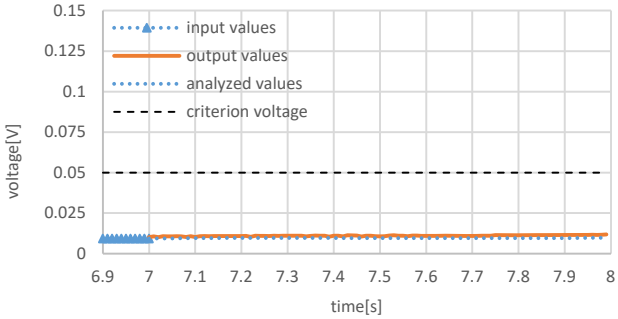

(a)

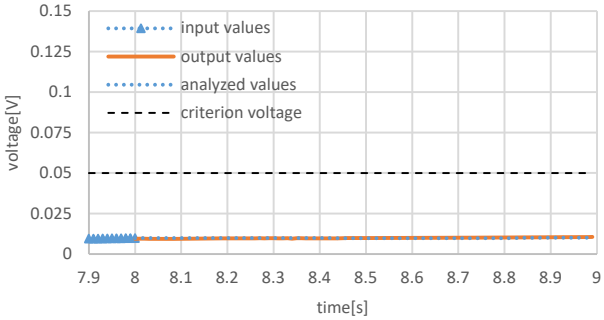

(b)

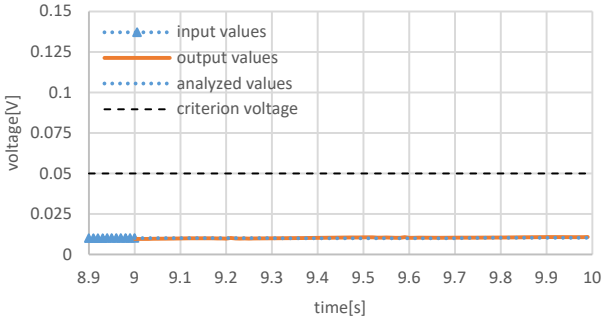

(c)

Fig. 7. Prediction for a not-quench case.

7762, pp. 496–499, 2019.
[10]Z. S. Hartwig, et al., "The SPARC toroidal field model coil program," submitted.
[11]A. Sagheer, M. Kotb, "Time series forecasting of petroleum production using deep LSTM recurrent networks," *Neurocomputing*, vol. 323, Jan. 2019. p.203-213.
[12]V. K. R. Chimmula, L. Zhang, "Time series forecasting of COVID-19 transmission in Canada using LSTM networks," *Chaos, Solitons Fractals*, vol. 135, Jun. 2020, Art. no. 109864.
[13]S. Siami-Namini, N. Tavakoli and A. Siami Namin, "A Comparison of ARIMA and LSTM in Forecasting Time Series," *2018 17th IEEE International Conference on Machine Learning and Applications*, Orlando, FL, USA, 2018, pp. 1394-1401.
[14]S. Noguchi, "Electromagnetic, Thermal, and Mechanical Quench Simulation of NI REBCO Pancake Coils for High Magnetic Field Generation," *IEEE Trans. Appl. Supercond*., vol. 29, no. 5, 2019, Art. no. 4602607.
[15]H. Ueda et al., "Numerical Simulation on Magnetic Field Generated by Screening Current in 10-T-Class REBCO Coil," *IEEE Trans. Appl. Supercond*., vol. 26, no. 4, 2016, Art. no. 4701205.
[16]M. T. Gonzalez, *et al*., "Normal-superconducting transition induced by high current densities in $YBa_2Cu_3O_{7-\delta}$ melt-textured samples and thin films Similarities and differences," *Phys. Rev. B 68*, 054514, Aug. 2003.
[17]W. T. B. de Sousa, A. Polasek, C. F. T. Matt and R. de Andrade, "Recovery of Superconducting State in an R-SCFCL MCP-BSCCO-2212 Assembly," *IEEE Trans. Appl. Supercond*., vol. 23, no. 1, Feb. 2013, Art. no. 5601407.
[18]L. Ren, *et al.*, "A Data-Driven Auto-CNN-LSTM Prediction Model for Lithium-Ion Battery Remaining Useful Life," *IEEE Trans. Industrial Informatics*, vol. 17, no. 5, May. 2021, pp. 3478-3487.
[19]J. Li, A. Mohamed, G. Zweig and Y. Gong, "LSTM time and frequency recurrence for automatic speech recognition," *2015 IEEE Workshop on Automatic Speech Recognition and Understanding*, Scottsdale, AZ, USA, 2015, pp. 187-191.
[20]M. A. Istiake Sunny, M. M. S. Maswood and A. G. Alharbi, "Deep Learning-Based Stock Price Prediction Using LSTM and Bi-Directional LSTM Model," *2020 2nd Novel Intelligent and Learning Emerging Sciences Conference*, Giza, Egypt, 2020, pp. 87-92.

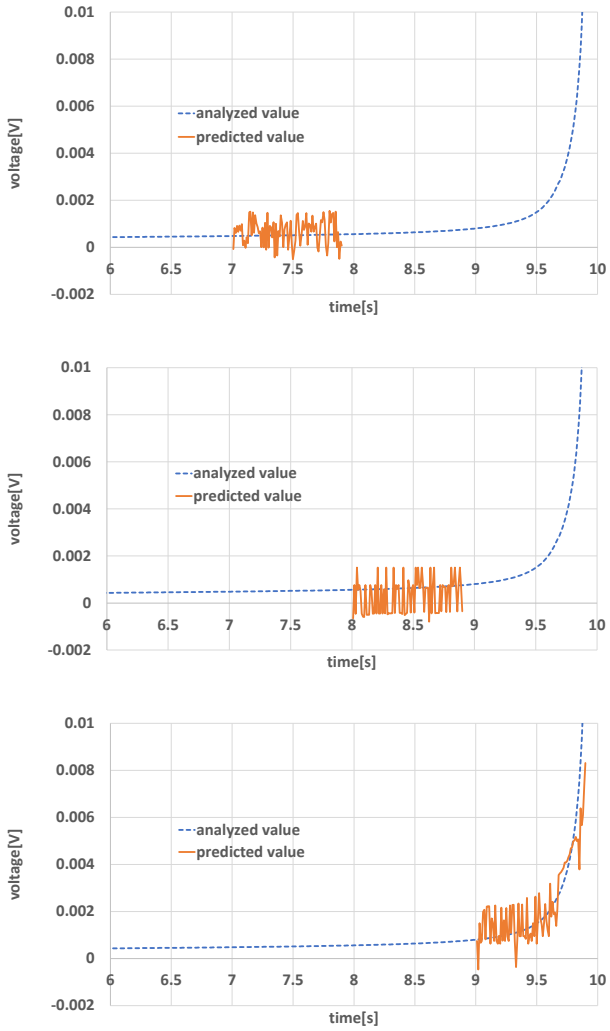

Fig. 6. Prediction for a quench case. (original ver.)

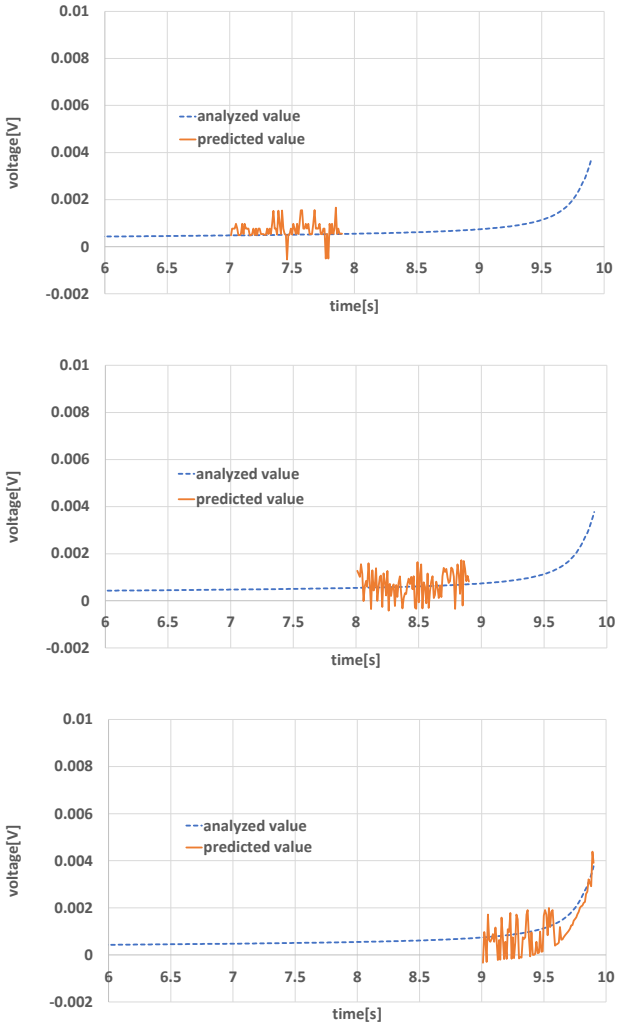

Fig. 7. Prediction for a not-quench case. (original ver.)